Neuron, Vol. 16, 35–46, January, 1996, Copyright ©1996 by Cell Press

Neuroglia and Pioneer Neurons Express UNC-6 to Provide Global and Local Netrin Cues for Guiding Migrations in C. elegans

William G. Wadsworth,* Harshida Bhatt,† and Edward M. Hedgecock‡

*Department of Pathology
Robert Wood Johnson Medical School
Piscataway, New Jersey 08854
†Roche Institute of Molecular Biology
Nutley, New Jersey 07110
‡Department of Biology
Johns Hopkins University
Baltimore, Maryland 21218

Summary

Netrins are laminin-related proteins that guide circumferential migrations on the ectoderm. To understand how netrin cues direct cell movements, we examined the expression of nematode netrin UNC-6 from embryo to adult. UNC-6 is expressed in 12 types of neuroglia and neurons, creating a hierarchy of netrin cues in the developing nervous system. Comparing gene expression pattern with in vivo phenotypes, we suggest how multiple netrin cues, each with a characteristic role, guide cells and axons during development. We also present the molecular analysis of selective loss-of-function and null alleles. The results indicate that the biological activities of netrins are mediated through distinct protein domains. Subtle mutations in domain VI can produce selective defects in both direction- and tissue-specific guidance. EGF-like module V-2 is essential for dorsal guidance activity; we infer this module is important for interactions between UNC-6 and the dorsal guidance receptor UNC-5.

Introduction

In the nematode Caenorhabditis elegans, cell surface and matrix proteins that provide directional cues for cell and axon migrations have been identified by genetic methods (Hedgecock et al., 1987; Wadsworth and Hedgecock, 1992). In particular, the gene *unc-6* is required to guide pioneer axons and mesoblasts in dorsal or ventral directions on the body wall (Hedgecock et al., 1990). The predicted product, designated UNC-6, is a secreted protein of 591 amino acids with an N-terminus homologous to laminin subunits and a unique C-terminus (Ishii et al., 1992). A simple model is that UNC-6 copolymerizes with laminin in the basement membrane to form a stable dorsoventral gradient that guides circumferential migrations on the body wall (Ishii et al., 1992). A cell surface receptor of the immunoglobulin superfamily, UNC-5, mediates some cellular responses to the UNC-6 guidance cue. In particular, UNC-5 expression in a motile cell is both necessary and sufficient for dorsal movements along the UNC-6 cue (Leung-Hagesteijn et al., 1992; Hamelin et al., 1993).

Recently, vertebrate orthologs of UNC-6, designated *netrin-1* and *netrin-2*, have been identified as chemoattractants and -repellents for developing axons in the embryonic nervous system (Serafini et al., 1994; Tessier-Lavigne et al., 1988; Kennedy et al., 1994; Colamarino and Tessier-Lavigne, 1995). Purified or recombinant netrin can promote and guide the outgrowth of axons *in vitro*, attracting or repelling their growth cones from some distance. In the developing nervous system, *netrin-1* mRNA is expressed in floor plate cells, while *netrin-2* mRNA is expressed in the ventral two-thirds of the spinal cord in regions flanking the floor plate.

The modular organization of netrins, which is conserved from nematodes to chordates, has several implications for their biological activities (Ishii et al., 1992; Serafini et al., 1994). N-terminal domains VI and V are homologous to laminin subunits α, β, and γ (Figure 1). Laminin molecules, which are heterotrimers of all three subunits, self-assemble via their domains VI, forming a stable polymeric scaffold for the basement membrane (Schittny and Yurchenco, 1990; Yurchenco and Cheng, 1993). This process is regulated by both calcium ions and proteoglycans. By inference, domain VI of netrins could allow their incorporation into basement membranes by copolymerization with laminin. Several epidermal growth factor (EGF)–like modules in domains V and III of laminin subunits are proposed to form binding sites for integrins and other cellular receptors (Beck et al., 1990; Hynes and Lander, 1992). By inference, netrin modules V-1, V-2, or V-3 might be the ligands for receptors on growth cones and migrating cells that respond to netrin cues. Finally, the basic domain at the C-terminus could tether netrin to other molecules for display on cell surfaces or unique matrix sites.

In this paper, we first describe the expression of nematode netrin UNC-6 from embryo through adult. We propose changing patterns of netrin expression provide a hierarchy of guidance cues throughout the ectoderm that are used in forming the basic axon scaffold of the nervous system and directing mesoblast movements on the body wall. To wit, along the body, ventral epidermoblasts and their descendants create a global netrin cue peaking near the midline of the body wall. Within the ventral nerve cord, midline neurons provide decussation cues, while pioneer axons provide unilateral cues to enhance left/right asymmetry. Sheaths provide netrin-labeled pathways in the nerve ring and labial nerves. From bilateral ganglia, pioneer axons provide netrin-labeled pathways into the nerve ring and ventral cord. A midline pioneer provides netrin-labeled pathways within the pharynx. This hierarchical model of UNC-6-mediated guidance integrates known genetic and anatomical data, reconciling several previously paradoxical observations, and makes specific predictions for experimental tests using microsurgery, genetic mosaics, and misexpression techniques.

Second, we describe protein structural changes that provide insights into how netrins may assemble and function at the macromolecular level. The *unc-6* gene was first identified and cloned using two, independent transposon-insertion mutants (Ishii et al., 1992). We have

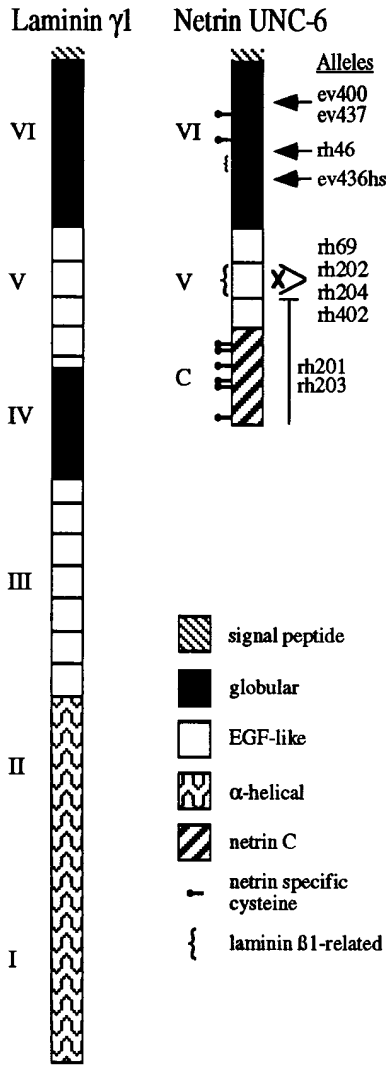

Figure 1. Modular Organization of Netrin

The N-terminus has a typical signal peptide followed by laminin-related domains VI and V. Domain V has three EGF-like modules, designated V-1, V-2, and V-3, arranged in tandem. The modular organization of a laminin γ subunit is shown for comparison. The basic domain at the C-terminus (C) has been found only in UNC-6 and other netrins (Serafini et al., 1994). The approximate positions of various *unc-6* mutations (described in text) are also shown. (After Ishii et al., 1992.)

determined the DNA and mRNA alterations in ten additional mutants, focusing on selective loss-of-function alleles that could be informative for relating netrin structure and function (Hedgecock et al., 1990). Each mutation examined causes a protein structural change in domains VI (residues 1–268), V (residues 269–437), or C (residues 438–591) of UNC-6 (Figure 1).

Our findings provide in vivo evidence that phyletically conserved cellular and molecular mechanisms underlie the development of the basic axon scaffold of the nervous system. At the cellular level, epidermal cells support and guide pioneer growth cones in the nematode body, while sheath cells may assume this role in the head. Based on their morphology and proposed function in the neurula, we suggest that nematode sheaths are related to the radial glia of chordates and similar, columnar neuroepithelial cells of other phyla (Jacobson, 1991). At the molecular level, netrin produced by epidermal cells and their descendants acts bifunctionally, e.g., as a chemoattractant for ventral migrations but as a repellent for dorsal migrations. In particular, the receptor UNC-5 helps to guide cells and growth cones away from UNC-6 concentrations. The mutant studies show that direction- and tissue-specific guidance activities are mediated by distinct netrin domains.

Results and Discussion

Epitope-Tagged UNC-6 Rescues *unc-6* Mutants

To monitor UNC-6 expression, we introduced an epitope-tag into the cloned *unc-6(+)* gene just following the predicted signal peptide. Following microinjection into oogonia of the null mutant *unc-6 (ev400)*, we recovered a homozygous strain carrying this transgene integrated at an unlinked chromosomal site. The integrated transgene, *unc-6::HA (urIs1),* fully rescues all mutant phenotypes, indicating that the epitope-tagged protein, UNC-6::HA, is both functional and nontoxic. Strains homozygous for *unc-6::HA (urIs1)* alone, obtained by outcrossing with wild-type males, are also fully wild type. We conclude that the integrated transgene causes no dominant phenotype, e.g., from misexpression, nor disrupts any visible gene. Embryos and larvae of both strains were examined by immunochemical methods.

The expression of the endogenous *unc-6* gene was inferred from these results. Since the mutant phenotypes are rescued, the transgene must be expressed in cells that would normally express the endogenous gene. Absent or ectopic misexpression of the transgene in a subset of cells would likely cause a mutant phenotype; however, this has not been tested. Other experimental data and observations that substantiate the expression patterns are also presented.

Netrin expression is complex and dynamic (Table 1). In the hermaphrodite, a total of 48 ectodermal cells, representing 12 cell types, express UNC-6::HA during either embryonic or larval development. In expressing cells, UNC-6::HA is generally detectable throughout the cytoplasm and processes, excluding the nucleus. By inference, it later appears on the surface of these cells or surrounding matrix. From its structure, secreted netrin could copolymerize with laminin in the basement membrane or, perhaps, assemble with unknown molecules for display on cell surfaces (Ishii et al., 1992). Unfortunately, we could not trace the fate of the epitope-tagged protein by immunofluorescence microscopy after its secretion. Presumably, the concentrations of netrin on the cell surfaces and extracellular matrix are too low for detection by these methods; or else, the N-terminal HA-epitope becomes masked when UNC-6 polymerizes via its domain VI (Schittny and Yurchenco, 1990).

Early Expression by Ventral Epidermoblasts

Ventral epidermoblasts P1/2-P11/12 are the first cells to express UNC-6::HA during embryogenesis. Netrin becomes detectable in the cytoplasm of these twelve cells

Table 1. Summary of UNC-6 Expression and Proposed Guidance Functions

Expression Period and Cell Types	Locations	Functions
Late gastrula to early neurula		
Epidermoblasts		
P1/2–P11/12	Ventral body wall	Ventral cord pioneers and motor axons
Early neurula to 3-fold neurula		
Sheaths		
CEPshVL, CEPshVR[1]	Ventral cephalic sensilla	Nerve ring pioneers
ILshDL, ILshDR, ILshL, ILshR, ILshVL, ILshVR	Inner labial sensilla	Labial nerve pioneers
Midline neurons		
I5	Pharynx	Head mesoblasts and pharyngeal tracts
PVT	Preanal ganglion	Guidepost
3-Fold neurula to adult		
Midline neurons		
AVG	Retrovesicular ganglion	Guidepost and right longitudinal tract
RIFL[2]	Retrovesicular ganglion	Right longitudinal tract
Bilateral neurons		
AVAL, AVAR	Lateral ganglia	Lateral pathway into nerve ring
AVBL, AVBR	Lateral ganglia	Ventral pathway into nerve ring
PVQL, PVQR	Lumbar ganglia	Pathway into preanal ganglion
First larval molt to adult		
Motorneurons		
VA2-VA12[3]	Ventral nerve cord	Gonadal mesoblasts and postembryonic neurons
VB3-VB11[4]	Ventral nerve cord	Gonadal mesoblasts and postembryonic neurons

[1] CEPshDL and CEPshDR do not express UNC-6.
[2] RIFR does not express UNC-6.
[3] VA1 does not express UNC-6.
[4] VB1 and VB2 do not express UNC-6.

soon after their births (circa 230 min) and before they form into regular rows (Figures 2A and 7). This staining gradually decreases in intensity as the cells spread ventrally, forming two symmetrical rows. At the completion of neurulation, soon after these rows have come together along the ventral midline, cytoplasmic staining is no longer detectable.

In *unc-6* mutants, widespread defects in circumferential migrations on the body wall likely reflect the absence of this major netrin cue (Hedgecock et al., 1990). Evidently, netrin is secreted as these epidermoblasts slide over the neuroectoderm and meet together along the ventral midline. We suggest that some or all of this netrin copolymerizes with laminin in the basement membrane to create a stable gradient of UNC-6 on the body wall that peaks near the ventral midline (see Figure 7). This gradient acts as an attractive cue for AVG and PVP growth cones as they pioneer the longitudinal tracts, and as a repulsive cue for DA, DB, and DD growth cones as they grow away from the ventral midline.

Expression by Sheaths in the Developing Head

All six inner labial and both ventral cephalic sheaths express UNC-6::HA in the early neurula. Netrin becomes detectable in these cells soon after their births (circa 310 min). At this time, the inner labial sheaths are clustered together just anterior to the developing pharynx (Figure 2B). As the head depression forms around comma-stage, the cell bodies move anteriorly toward the sensillar rudiments, revealing processes trailing back to the developing nerve ring. The endfeet form a more-or-less complete path around the pharynx that anticipates the anterior margin of the nerve ring. UNC-6::HA is detectable along the entire cell body and process at this time (Figures 2C and 2D). As the embryo elongates, the cell bodies initially stay near the sensillar rudiments at the tip of the head. Presently, as judged by UNC-6::HA staining, the processes no longer reach the developing nerve ring. By inference, they fail to stretch apace with the rapid elongation of the head. As the pharynx elongates, the cell bodies assume their mature positions (Sulston et al., 1983), typically just anterior or posterior to the metacorpus (Figures 3A and 3B). Netrin expression is transient; only weak staining of UNC-6::HA is detectable in these cells beyond 3-fold elongation. The sheath processes appear to provide a scaffold of netrin-labeled pathways that support and guide labial axons to the nerve ring. Moreover, their endfeet could form a ring-shaped substratum for axons within the ring itself.

The cephalic sheaths are positioned dorsally and ventrally just anterior to the developing nerve ring (Sulston et al., 1983). In the early neurula, these cells extend sheetlike processes that apparently anticipate the outer surface of the ring neuropil. At this time, UNC-6::HA is detectable throughout the cell body and processes of the ventral cephalic sheaths (Figures 2B–2D). Netrin expression is transient; UNC-6::HA is no longer detectable in these cells by 3-fold elongation. Finally, no UNC-6::HA expression is ever observed in the dorsal cephalic sheaths. Conceivably, the dorsal cephalic sheaths express another unknown molecular cue that complements UNC-6 in guiding pioneer axons around the developing ring. Pioneers entering the ring neuropil from the ventral and lateral ganglia, for example, could be guided

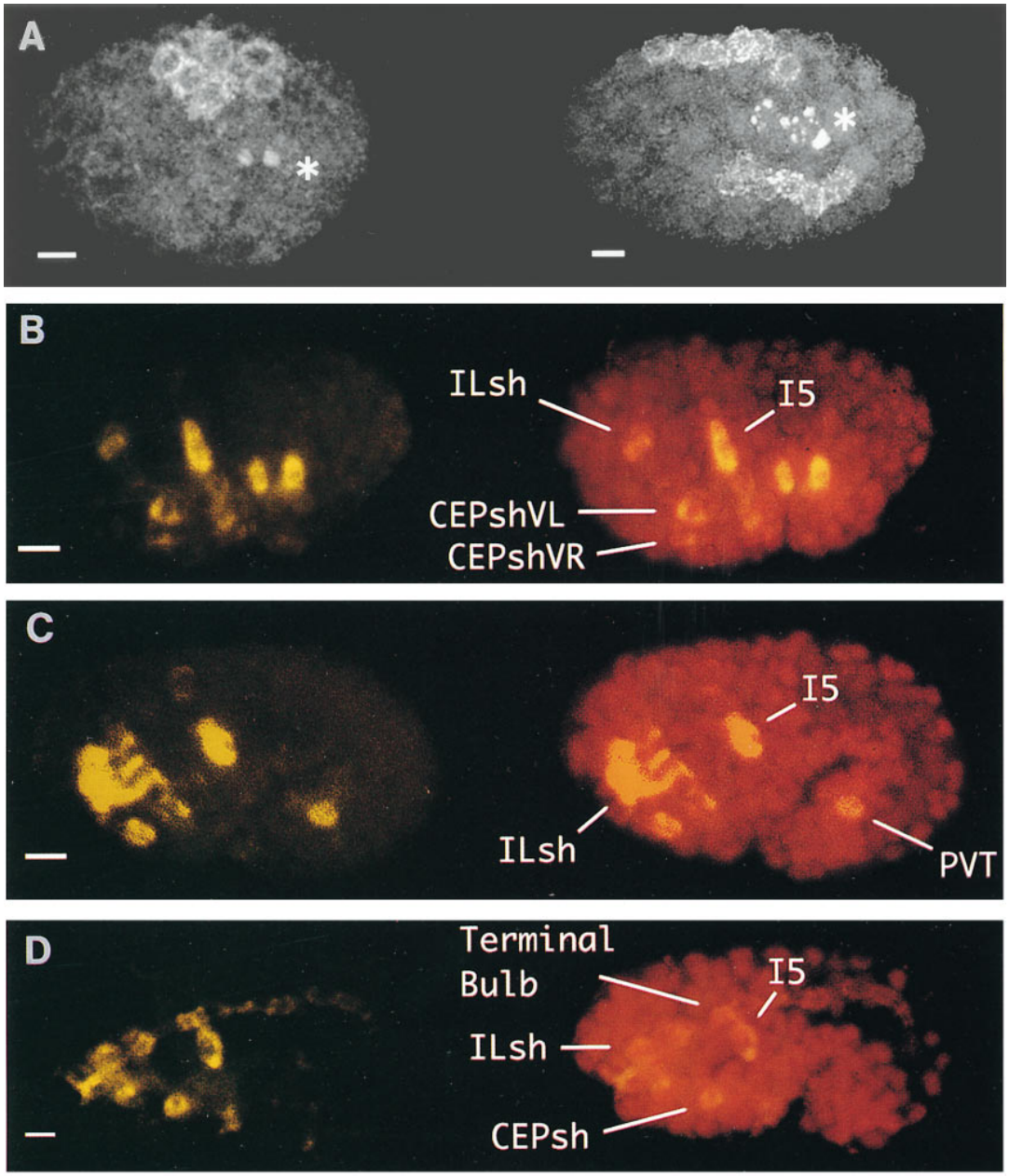

Figure 2. Confocal Micrographs of UNC-6::HA Staining in Early Embryos

Anterior is shown on the left. Scale bars, 5 μm. (A) Ventral horizontal plane showing netrin expression during neurulation when the ventral epidermoblasts P1/2-P11/12 spread ventrally to enclose the embryo (230–290 min). For landmarks, these embryos were costained with mAb OIC1D4, which recognizes cytoplasmic granules (asterisks) in germline cells positioned on the ventral midline. (left panel) About 250 min: in late gastrula, the ventral epidermoblasts form two groups of six cells on either side of the embryo. In this plane, bright cytoplasmic staining is visible within all six cells of the left group. (right panel) About 280 min: midway through neurulation, the ventral epidermoblasts have formed into two regular rows converging toward the midline. (B–D) Midsagittal planes showing netrin expression in early neurulae. (left panels) UNC-6::HA is shown in yellow. (right panels) Anaglyph with cell nuclei shown in red (propidium iodide stain). (B) About 340 min: inner labial (ILsh) and ventral cephalic sheath cells (CEPshV) are visible in the head. Neuroblast I5 is visible within the developing pharynx. Ventral epidermoblasts are still visible in the body. (C) About 430 min: the sheaths have moved anteriorly, leaving a scaffold of netrin-labeled processes underlying the developing nerve ring and labial nerves. Neuron PVT is now visible in the preanal region, while the ventral epidermoblasts are no longer detectable in the body. (D) About 415 min: within the terminal bulb of the pharynx, neuron I5 is visible just ventral to the adherens junctions that anticipate the pharyngeal lumen. For landmarks, this embryo was costained with mAb MH27, which recognizes adherens junctions in the pharynx and other epithelia.

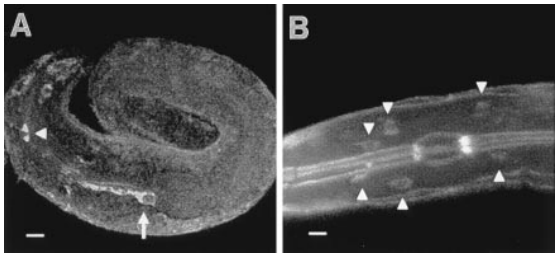

Figure 3. Confocal Micrographs of UNC-6::HA Staining in the Late Embryo

Anterior is shown on the left. Scale bars, 5 μm.
(A) About 3-fold elongation: several inner labial sheaths are visible near the sensilla at the tip of the head, but one cell (arrowhead) has already moved posteriorly toward its mature position. Within the pharynx, the cell body (arrow) and paired axons of neuron I5 are visible on the ventral midline of the epithelium.
(B) About 4-fold elongation: the inner labial sheaths (arrowheads) are faintly visible near their mature positions immediately anterior or posterior the metacorpus of the pharynx. For landmarks, this embryo was costained with mAb MH27.

by attractive cues from the ventral or dorsal sheaths, respectively (see Figure 7).

The importance of UNC-6 cues in the developing nerve ring is still uncertain. A handful of sensory neurons in the lateral ganglia were previously examined in *unc-6* mutants by fluorescein isothiocyanae (FITC)–filling (Hedgecock et al., 1990). The trajectories of these axons through the amphid commissures and nerve ring appeared normal. Conceivably, some UNC-6 cues in the nerve ring, important for ancestors with a larger nervous system, are merely vestigial. Alternatively, a second, unknown molecular cue in the nerve ring may render the UNC-6 cues more-or-less redundant. Finally, subtle or impenetrant defects in the amphidial axons could easily have been overlooked due to the limitations of the labeling technique. In any case, the development of the nerve ring in *unc-6* mutants deserves a closer examination using improved reporters and additional neuron types.

Expression by Midline and Asymmetric Neurons in the Developing Nerve Cord

Positioned at the anterior and posterior ends of the developing ventral nerve cord, respectively, the midline neurons AVG and PVT express UNC-6::HA (Table 1). Netrin becomes detectable in the PVT neuron soon after its birth (circa 290 min). At this time, PVT is positioned on the ventral midline of the body wall just anterior to the developing rectum (Figure 2C). Netrin expression is transient; UNC-6::HA is no longer detectable in this cell by 3-fold elongation. By then, PVT has shifted to its mature position as the most anterior cell in the preanal ganglion. Born circa 290 min, AVG does not express UNC-6::HA until about 3-fold elongation. AVG is positioned on the ventral midline in the retrovesicular ganglion at this time (Figure 4A). Netrin expression then continues through the larval and adult stages.

The early development of the ventral nerve cord has been traced by serial electron microscopy (EM) reconstruction of staged embryos (Durbin, 1987). From the retrovesicular ganglion, the midline neuron AVG extends the first axon posteriorly along the ventral nerve cord (see Figure 7). This axon invariably pioneers the right tract of the nerve cord. After reaching the preanal ganglion (circa 480 min), it continues along the rectal epidermis to the dorsorectal ganglion. From about 480 to 520 min, the motorneurons DA, DB, and DD extend axons dorsally to establish the dorsal nerve cord. During the same period, the paired neurons PVP in the preanal ganglion extend axons anteriorly along the nerve cord. These axons first decussate at the ventral midline, and then pioneer the contralateral tract. The paired neurons PVQ in the lumbar ganglia pioneer the lumbar commissures to the preanal ganglion where they fasciculate with the PVP axons and travel anteriorly in the ipsilateral tract. Finally, the paired neurons RIF in the retrovesicular ganglion extend axons anteriorly toward the developing nerve ring. Like PVP in the preanal ganglion, these axons first decussate at the ventral midline, and then pioneer the contralateral tracts.

Midline neurons AVG and PVT are cellular landmarks expressing UNC-6 at the anterior and posterior ends of the ventral nerve cord, respectively. One likely function of these netrin cues is to guide pioneer axon decussation at the ventral midline. To test this idea, the axons of ventral nerve cord pioneers PVPL and PVPR were examined by immunofluorescence microscopy. In wild type, these neurons are situated symmetrically in the preanal ganglion just posterior to PVT (Figures 5A and 5B). Their axons first decussate at the ventral midline, and then pioneer the contralateral tracts of the ventral nerve cord. In *ev400*, an *unc-6* null allele, one of the two axons fails to decussate and travels instead in the ipsilateral tract of the ventral nerve cord, in about 30% of the larvae (Figure 5C). More rarely, an axon leaves the ventral nerve cord entirely and travels anteriorly along the lateral epidermis. The frequencies and spectra of PVP defects in *unc-40 (e271)* and *ev437*, an *unc-6* allele that selectively disrupts ventral guidance, are similar to *unc-6 (ev400)*. The frequencies of PVP defects in *e78* and *rh68*, *unc-6* alleles that partially disrupt both ventral and dorsal guidance, are significantly lower. Finally, no PVP defects were observed in either *unc-5 (e53)*, or *rh69*, *rh202*, *rh204*, and *rh402*, *unc-6* alleles that exclusively disrupt dorsal guidance.

An UNC-6 cue on the surface of the PVT neuron in the preanal ganglion is proposed to position the pioneer neurons PVP and guide their axons during decussation. Moreover, the UNC-6 cue from the ventral epidermoblasts prevents the PVP growth cones from straying from the midline as they grow along the longitudinal tracts. As predicted, the cell bodies and axons of the PVP neurons are frequently misplaced in *unc-6* mutants. The effects of ablating the PVT neuron have not been described. Interestingly, PVT is purely a guidepost neuron since its cell body, and not its axon, is important in ventral cord development. Indeed, the mature neuron has only a short axon and no synaptic outputs, suggesting it plays no role in the completed circuit (White et al., 1986).

Besides AVG, a second neuron in the retrovesicular ganglion, RIFL (born circa 410 min), also expresses UNC-6::HA from about 3-fold elongation through adult (see Figure 4A). Interestingly, no UNC-6::HA expression

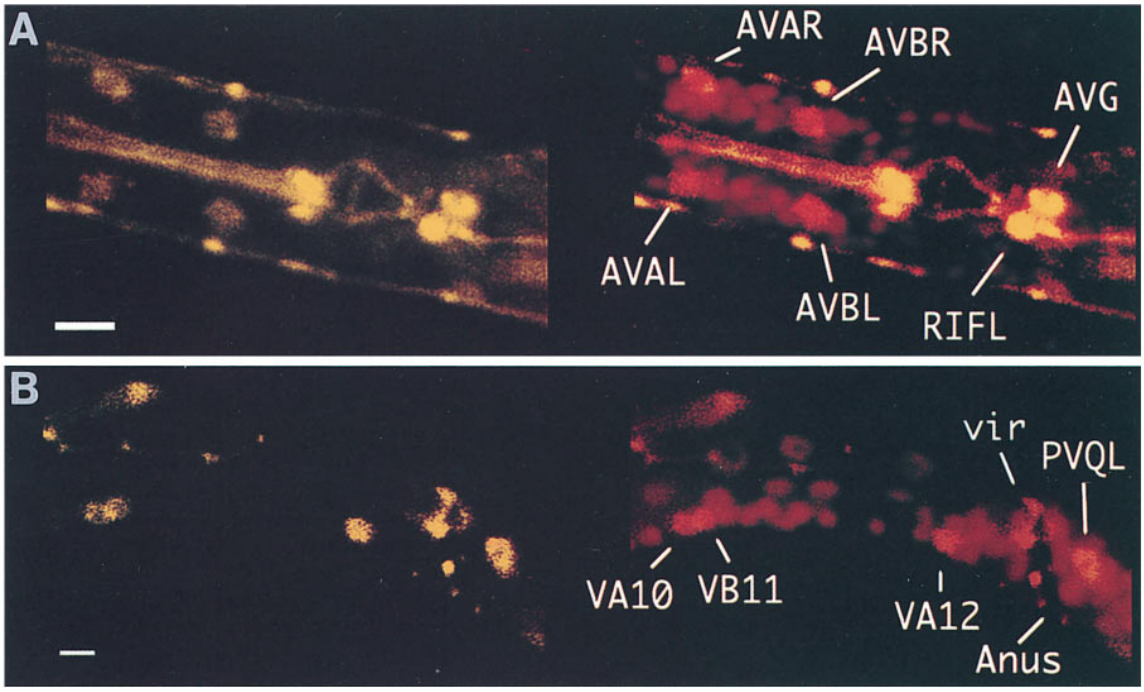

Figure 4. Confocal Micrographs of UNC-6::HA Expression in the Larva

Anterior is shown on the left. Scale bars, 5 μm. (left panels) UNC-6::HA is shown in yellow. For landmarks, these larvae were costained with mAB MH27. (right panels) Anaglyph with cell nuclei shown in red (propidium iodide stain).

(A) Lateral horizontal plane of head showing nerve ring and retrovesicular ganglion. Neurons AVG and RIFL are visible in the retrovesicular ganglion at the anterior end of the ventral nerve cord. Paired neurons AVA and AVB are visible in the lateral ganglia of the nerve ring. Adherens junctions in the phayrnx and body wall are stained by mAb MH27.

(B) Midsagittal plane of tail showing preanal region and left lumbar ganglion. Motorneurons VA10, VA12, and VB11 are visible in the ventral nerve cord, while VA11 is visible in an adjacent plane (not shown). Between the preanal and lumbar ganglia, the rectum itself is devoid of cell nuclei. Atop the rectum, adherens junctions in the intestinorectal valve cells (vir) are stained by mAb MH27. Neuron PVQL is visible in the left lumbar ganglion.

is ever observed in the bilateral homolog RIFR. Together, the AVG and RIFL axons could provide a continuous netrin-labeled pathway restricted to the right tract of the nerve cord. This unilateral cue could guide the nonreciprocal decussation of various paired axons from the nerve ring (e.g., AVA, AVB) and lumbar ganglia (e.g., PVC), as they enter the ventral nerve cord, and promote cohesion of axons within the cord itself. If the parent of AVG is ablated in wild-type embryos, interneurons and ventral cord motorneurons form several small fascicles rather than one coherent right longitudinal tract (Durbin, 1987). Moreover, these axon fascicles are sometimes misplaced to the left of the ventral midline. Conceivably, ablation of AVG and RIFL together would produce a more expressive and penetrant defect. Similar, but less pronounced, defects have been described in the ventral nerve cord of *unc-6* mutants (Hedgecock et al., 1990). A strong bias of axons toward the right tract persists even in *unc-6* null mutants. Evidently, the netrin cues provided by AVG and RIFL axons merely amplify an underlying asymmetry of the ventral epidermis that does not itself require UNC-6 expression.

Expression by Lateral Ring and Lumbar Ganglia Neurons

Paired neurons AVA, AVB, and PVQ express UNC-6::HA in the lateral and lumbar ganglia, respectively (Table 1). Born circa 300 min, netrin does not become detectable in these cells until about 3-fold elongation. Netrin expression then continues through the larval and adult stages. The AVA neurons are the most anterior cells in the lateral ganglia, whereas the AVB neurons are among the most posterior (see Figure 4A). There is some ambiguity in identifying the second pair of antibody-labeled cells as AVB by these methods. Adjacent to AVB in the lateral ganglia, the motorneurons RIM are a plausible alternative assignment. Finally, the PVQ neurons are the most anterior cells in the lumbar ganglia in the tail (see Figure 4B).

The pioneer neurons PVQ in the lumbar ganglia may follow the UNC-6 cues from the ventral epidermoblasts and PVT to the preanal ganglion where their axons fasciculate and travel alongside the PVP axons (see Figure 7). After axogenesis begins, PVQ itself expresses UNC-6. This netrin cue in the lumbar commissures could guide later axons to the ventral nerve cord. When the parent of PVQ is ablated in wild-type embryos, later axons from the lumbar ganglia may fail to reach the ventral nerve cord (Durbin, 1987). Similarly, in *unc-6* mutants, some or all lumbar axons may fail to reach the ventral nerve cord (Hedgecock et al., 1990).

We propose that AVA and AVB pioneer the lateral and ventral routes, respectively, from the lateral ganglia into the nerve ring (see Figure 7). These axons may be guided

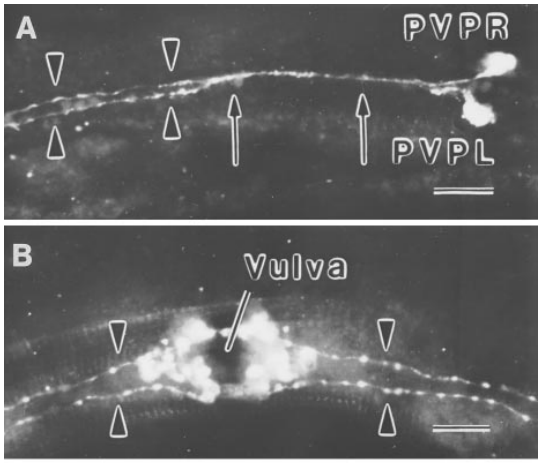

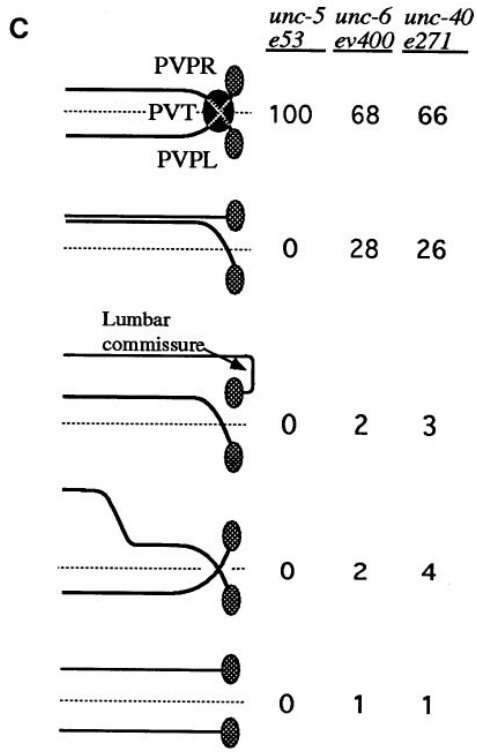

Figure 5. Immunofluorescence Micrographs of the PVP Neurons and Summary of PVP Neuron Defects

(A–B) Ventral aspect of fourth-stage hemarmaphrodite larva stained with monoclonal antibody M44. Scale bars, 10 μm.

(A) Preanal region showing cell bodies and axons of pioneer neurons PVPL and PVPR. In the neurula, these axons decussate at the ventral midline and then pioneer the contralateral tracts of the ventral nerve cord (White et al., 1986). In the mature preanal neuropil, the region of contact between PVPL and PVPR axons is more extensive (arrows). Beyond the preanal ganglion, the longitudinal tracts of the ventral nerve cord are well separated (arrowheads).

(B) Midbody region showing PVP axons (arrowheads) traveling on either side of the developing vulva. The attachments of vulval muscles to the epidermis, which also stain with mAb M44, are visible.

(C) The PVP neurons were examined by immunofluorescence microscopy in fourth-stage hermaphrodites stained with mAb M44 (n = 100). Data for PVPL and PVPR axons are pooled; frequencies of defects were comparable for both cells. Two additional defects (not shown) were observed in individuals with otherwise normal axons. First, one or both PVP cell bodies was significantly displaced in 10/68 *unc-6* and 6/66 *unc-40* larvae. Second, one of the PVP neurons was bipolar, extending both an anterior and a posterior axon, in 3/68 *unc-6* and 3/66 *unc-40* larvae. Monoclonal antibody M44 is a mouse IgG1, generated by immunization with C. elegans homogenates, that reacts with a cell surface antigen on the PVP neurons.

through the nerve ring by netrin and other cues provided by the cephalic sheaths. In particular, we suggest that AVA is first attracted and then repelled by UNC-6 from the ventral sheaths. Conversely, AVB is first repelled and then attracted to this same netrin cue. After axogenesis begins, the neurons AVA and AVB themselves express UNC-6. Hence, like PVQ in the lumbar ganglia, these pioneer axons could provide netrin-labeled pathways for guiding later axons to the nerve ring and ventral ganglion.

Expression by a Midline Neuron in the Developing Pharynx

The midline neuron I5 expresses UNC-6::HA in the developing pharynx (Table 1). Netrin becomes detectable in this cell soon after its birth (circa 280 min). Positioned on the ventral midline, I5 is the most posterior neuron in the pharynx at this time (Figures 2B and 2C). Netrin expression is transient; UNC-6::HA is no longer detectable in the cell body after about 3-fold elongation (see Figure 3A), but staining in the axons persists somewhat longer. We propose that I5 pioneers the ventral longitudinal tracts of the pharynx (Albertson and Thomson, 1976). These axons could provide netrin-labeled pathways for guiding later axons within the pharynx. Netrin from I5 might also copolymerize with laminin molecules in the basement membrane surrounding the pharynx to create a stable gradient of UNC-6 that peaks near the ventral midline. This netrin could act as a repulsive cue for guiding the head mesodermal cells, which are external to the pharynx, as they migrate dorsally around the terminal bulb (Hedgecock et al., 1990).

Excepting the observation that feeding is normal, the pharyngeal nervous system has not been examined in *unc-6* mutants (Hedgecock et al., 1990). Head mesodermal cells, which migrate dorsally on the basement membrane surrounding the pharynx, are affected in *unc-5* and *unc-6* mutants. We predict that removal of the I5 cues may disrupt both axon migrations within the pharynx and these mesoblast migrations outside the pharynx.

Expression by Larval Ventral Cord Motorneurons

Postembryonic motorneurons VA2–VA12 and VB3–VB11 express UNC-6::HA in the ventral nerve cord (Table 1). Netrin becomes detectable in these cells soon after their births at the end of the first larval stage. This expression continues through the adult stage (see Figure 4B). After hatching, the C. elegans larva increases about 5-fold in both length and circumference before becoming an adult. Netrins and other molecular cues incorporated into basement membranes during embryogenesis must

be greatly diluted during larval growth unless somehow augmented by new secretion. Six axons (AVAL, AVAR, AVBL, AVBR, AVG, and PVQR) in the right longitudinal tract and one axon (PVQL) in the left tract provide a continuous source of UNC-6 in the ventral nerve cord. Near the end of the first larval stage, the twenty postembryonic motorneurons (VA2–VA12, VB3–VB11) provide a further source of UNC-6 in the right tract. These motorneurons could maintain and sharpen the proposed gradient of netrin in the basement membrane of the epidermis and skew its peak farther to the right of the ventral midline.

Molecular Biology of *unc-6* Mutants

Both direction-specific (dorsal versus ventral) and tissue-specific (ectodermal versus mesodermal) guidance functions of *unc-6* are genetically separable, suggesting UNC-6 has multiple functional domains (Hedgecock et al., 1990; Wadsworth and Hedgecock, 1992). To better understand the molecular basis of these observations, we have characterized DNA and mRNA alteration of selective loss-of-function alleles that could be informative for relating netrin structure and function.

Alleles *ev400* and *rh46*, obtained through ethylmethanesulfonate mutagenesis, cause a complete loss of *unc-6(+)* functions, or null phenotype (Hedgecock et al., 1990). Allele *ev400* contains a GC-to-AT transition in codon Q78, near the beginning of domain VI, which introduces a UAA stop codon (Figure 6A). Allele *ev437* is a spontaneous pseudorevertant of *unc-6 (ev400)* that restores dorsal, but not ventral, guidance activity (Hedgecock et al., 1990). This mutation replaces the sequence TAA.TCC.CAT comprising codons 78–80 of *unc-6 (ev400)* by the sequence TCC.TCT. As a consequence, the reading frame of the mRNA is restored, shortened by one codon (Figure 6A).

Allele *rh46* contains a GC-to-CG transversion in codon A136, around the middle of domain VI, which substitutes a proline residue (Figure 6B). Allele *ev436* is a spontaneous pseudorevertant of *unc-6 (rh46)* that restores axonal, but not mesoblast, guidance activity (Hedgecock et al., 1990). The restored activity is heat-sensitive (unpublished data). Allele *ev436* contains a GC-to-AT transition in codon A193, near the end of domain VI, which substitutes a threonine residue (Figure 6B).

Five independent, apparently spontaneous, *unc-6* alleles were recovered from screening about 150,000 wild-type animals (Hedgecock et al., 1990). Two are null alleles, whereas the others disrupt dorsal, but not ventral, guidance activity. From Southern analysis, the null alleles *rh201* and *rh203* contain large deletions that extend downstream from intron 7 and remove exons 8–13. If these alleles produce a translatable mRNA, the mutant netrin must lack domains V-3 and C. Alleles *rh202* and *rh204* contain smaller deletions that extend upstream from intron 7 and remove exons 5–6. By Northern analysis and sequencing of polymerase chain reaction (PCR)–amplified cDNAs, these alleles produce an mRNA species, designated ΔExons6–7, in which exons 5 and 8 are spliced directly together (Figure 6C). This mRNA codes an inframe protein precisely lacking the second EGF-like module in domain V (residues 324–387). Allele *rh402* contains a small deletion that extends upstream from intron 7 and ends within exon 7. Again, the single mature mRNA species is the ΔExons6–7 splice product (Figure 6C).

The high rate of spontaneous deletion and tight clustering of break points suggests that *unc-6(+)* contains a sequence within intron 7 that promotes DNA breakage or recombination. Two unusual features of this region are a long poly-G tract and a repeated 17-mer, ATAAGAT TGGGGAAAAG (Ishii et al., 1992). The precise break points of deletions *rh202*, *rh204*, and *rh402* were determined by sequencing (Figure 6D). Each deletion is bounded by a short direct repeat (TA, TTCTAGAA, or TGCAAA) suggesting that the premutation, whatever its origin, is excised via imprecise recombination.

Finally, allele *rh69*, obtained through ethylmethanesulfonate mutagenesis, selectively disrupts dorsal guidance activity (Hedgecock et al., 1990). It is phenotypically indistinguishable from the deletion alleles *rh202*, *rh204*, and *rh402* described above. Allele *rh69* contains an AT-to-TA transversion that disrupts the splice donor site of intron 6 (Figures 6C and 6D). Most mature mRNA in this mutant retains the unspliced intron, but the ΔExons6–7 species forms a minor, second product.

A Hierarchy of Netrin Cues

The UNC-6 expression pattern reveals how multiple netrin cues, each with a characteristic role, guide cells and axons in the developing nervous system. This pattern is complex, but we can discern five recurring themes. First, netrin expression is spatially restricted to the ventralmost cells within each region of the nervous system (Figure 7). In the body wall, for example, UNC-6 is expressed by ventral but not lateral epidermoblasts. In the nerve ring, UNC-6 is expressed by ventral but not dorsal cephalic sheaths. In both the pharynx and the ventral nerve cord, UNC-6 is expressed by ventral midline neurons. Such ventral restriction of netrin expression likely extends to all phyla (Kennedy et al., 1994).

Within the ventral nerve cord, UNC-6 expression is strongly biased to the right longitudinal tract. As axogenesis begins, the pioneer neurons AVG and RIFL provide a unilateral UNC-6 cue. An additional asymmetric source in the larva is provided by the postembryonic motorneurons VA and VB. Conceivably, unilateral netrin cues, so pronounced in nematodes, underlie some of the asymmetries observed in the nervous systems of other phyla.

Second, broadly distributed guidance cues are supplemented by more restricted ones as development proceeds. Moreover, the same molecular species can be used at each refinement. In the preanal region, for example, epidermoblasts P11/12L and P11/12R provide a global UNC-6 cue on the ventral body wall. Next, the guidepost neuron PVT provides a local UNC-6 cue at the ventral midline. Finally, the pioneer neurons AVG and PVQ provide pathways of UNC-6 into the preanal ganglion.

Third, mesodermal migrations are guided by netrin cues provided by ectodermal epithelia. Although UNC-6 guides various mesoblasts in the neurula and larva, it is never expressed by mesodermal derivatives. Ectodermal cells in the body wall and pharynx must provide

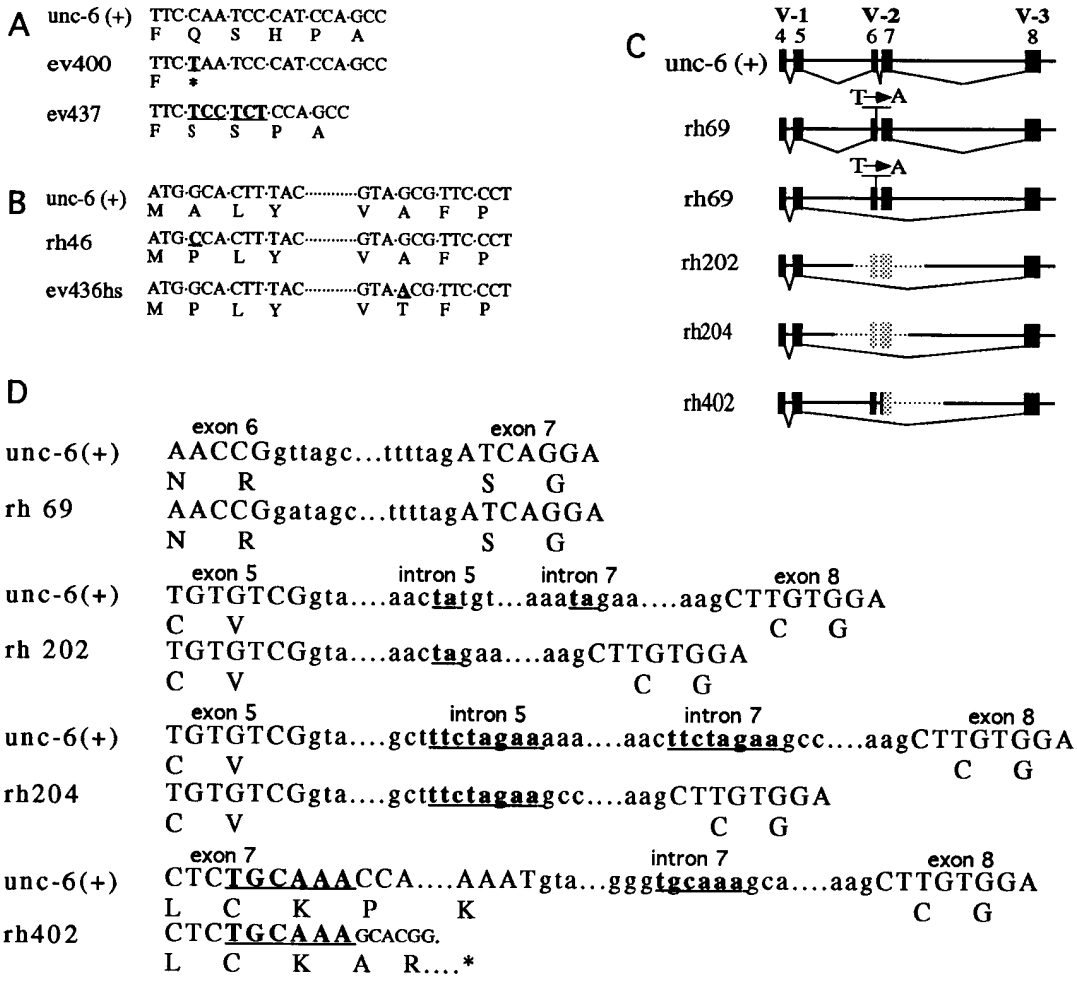

Figure 6. Molecular Biology of *unc-6* Mutants

(A) Codons 77–81 in *unc-6 (+)*, *unc-6 (ev400)* and *unc-6 (ev437)*.

(B) Codons 135–138 and 192–195 in *unc-6 (+)*, *unc-6 (rh46)* and *unc-6 (ev436)*. Alleles *ev400* and *rh46* cause complete loss of *unc-6 (+)* functions, whereas allele *ev437* causes loss of ventral, but not dorsal, guidance activity and allele *ev436* causes loss of mesodermal, but not axonal, guidance activity.

(C) Summary of mutations and spliced mRNA products produced by alleles of *unc-6* that selectively disrupt dorsal guidance activity. Exons 4–8 that encode the three EGF-like modules of domain V are shown as closed boxes and the splicing patterns are indicated by thin lines. The mutations in *unc-6 (rh69)*, *unc-6 (rh202)*, *unc-6 (rh204)*, and *unc-6 (rh402)*, and their consequences for mRNA splicing are shown. Genomic sequences deleted in mutant alleles are shaded and the transversion within a splice donor site of allele *rh69* is indicated.

(D) Sequence analysis of the splice donor site in intron 6 of *unc-6 (+)* and *unc-6 (rh69)* and the deletion break points in *unc-6 (rh202)*, *unc-6 (rh204)*, and *unc-6 (rh402)*. Direct repeats flanking the break points are underlined.

the UNC-6 cues for these migrations. By inference, this netrin is incorporated in the basement membranes of these epithelia that provide the actual substrata for mesoblast movement (Hedgecock et al., 1990; Wadsworth and Hedgecock, 1992).

Fourth, whether a netrin cue is attractive or repulsive depends upon the motile cell itself and, particularly, the current state of its navigational program. The global UNC-6 cue on the body wall provided by the ventral epidermoblasts and their descendants guides two-way traffic on the body wall (Figure 7). It acts as a repulsive cue for motorneurons DA, DB, and DD, but an attractive cue for various sensory and interneurons. It acts alternately as an attractive and a repulsive cue for the linker cell of the male gonad. Mutations in several regulatory genes alter the trajectories of these mesoblasts by reprogramming their responses to UNC-6 and other body wall cues (A. Antebi et al., personal communication). Similarly, the UNC-6 cue from the cephalic sheaths may act alternately as an attractive and a repulsive cue for nerve ring pioneers.

Finally, regardless of whether UNC-6 is acting as an attractant or repellent, additional adhesion molecules evidently provide the permissive substratum for cell movement (Hedgecock et al., 1990). Sensory axons in the labial nerves, for example, may be constrained to migrate along the processes of the inner labial sheaths by cell adhesion molecules. In this case, the proposed rostral–caudal gradient of UNC-6 along the process would determine the direction of migration.

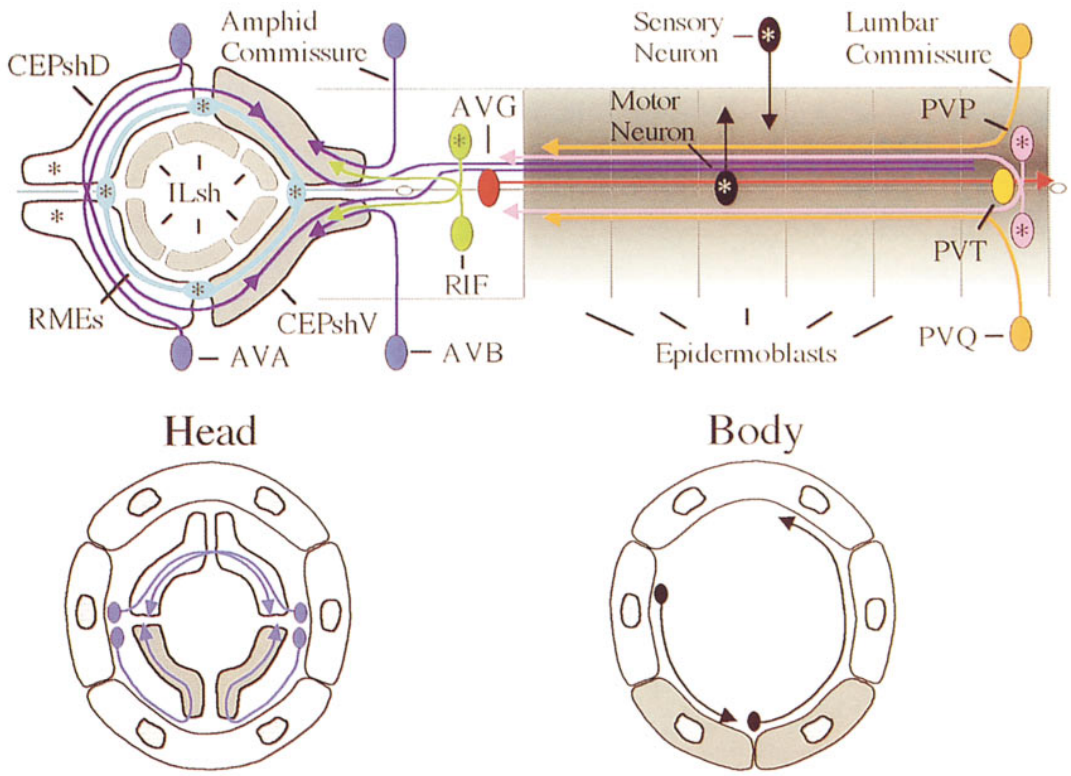

Figure 7. UNC-6 Expression and Functions in the Embryonic Ectoderm

(Top) The body wall is shown opened along the dorsal midline in cylindrical projection, while the nerve ring is flattened in anterior projection (cf. White et al., 1986). Excepting neuron I5 in the pharynx, all cells that express UNC-6 in the embryo are shown. Asterisks mark additional cells, included for reference, that do not express UNC-6. Neurons are located within various ganglia, i.e., lateral (AVA, AVB), retrovesicular (AVG, RIF), preanal (PVP, PVT), or lumbar (PVQ). The excretory pore and anus provide landmarks along the ventral midline.

Cephalic sheaths (CEPsh) support RME neurons and various axons within the ring neuropil. Inner labial sheaths (ILsh) guide axons entering the neuropil from the anterior via the six labial nerves. Cephalic sheaths guide axons entering the neuropil from the posterior via lateral (e.g., AVA) and ventral routes (e.g., AVB). AVA and AVB axons undergo reciprocal decussations at the dorsal midline of the ring.

Ventral epidermoblasts (P1/2-P11/12) support axons within the ventral nerve cord. Guidepost neurons AVG and PVT mark the anterior and posterior boundaries of the nerve cord proper. Neurons RIF and PVP undergo reciprocal decussations before pioneering the ventral longitudinal tracts. AVA and AVB axons undergo nonreciprocal decussations as they enter the nerve cord. PVQ axons pioneer the lumbar commissures and then travel alongside the PVP axons in the nerve cord.

(Bottom) The body wall and nerve ring are shown in cross-section. The ventral cephalic sheaths and ventral epidermoblasts, which express UNC-6, are filled. Axons of neurons AVA and AVB in the lateral ganglia enter the nerve ring by lateral and ventral routes, respectively. In the midbody, typical sensory and motor neurons are shown projecting to the ventral and dorsal nerve cords, respectively.

Attractive and Repulsive Roles Are Mediated by Distinct UNC-6 Domains

Comparison of protein structural changes with mutant phenotypes provides several insights into how netrins may assemble and function at the macromolecular level (see Figure 1). First, we have confirmed that *unc-6 (ev400)* and similar severe alleles represent the null phenotype of this gene. Null alleles *rh201* and *rh203* each delete exons 8–13, which encode netrin modules V-3 and C. Evidently, these deleted sequences are important for either gene expression or stability and activity of the gene products.

Second, missense and other subtle mutations in domain VI can produce at least two distinct selective loss-of-function phenotypes (Figures 6A and 6B). Allele *ev436*, for example, selectively disrupts mesoblast but not axonal migrations (Hedgecock et al., 1990). Conceivably, this mutation affects the display of UNC-6 on the outward face of the basement membrane, which contacts mesoblasts, but not its display on the inward face or cell surfaces, which contact neuronal growth cones. Allele *ev437* selectively disrupts ventral migrations of both axons and mesoblasts (Hedgecock et al., 1990). Conceivably, some distinct mechanism of tethering, affected by this mutation, is used to maintain a high concentration of netrin along the ventral midline.

Finally, we propose that the EGF-like module V-2 is essential for dorsal, but not ventral, guidance activity. Hitherto, no function has been assigned to this module in any laminin subunit or laminin-related protein. Four independent *unc-6* alleles with selective defects in dorsal migrations each produce an identical mutant protein that precisely lacks this module (Figures 6C and 6D). In particular, this module could provide a binding site for the dorsal guidance receptor UNC-5 (Leung-Hagesteijn et al., 1992; Hamelin et al., 1993). Less likely, the changed spacing between modules caused by the V-2 deletion could disrupt UNC-5 binding at another site. Interestingly, while netrins are generally more similar to the γ subunits, module V-2 shares the phyletically

conserved hallmarks of the V-2 module of laminin β subunits.

Experimental Procedures

General Methods

Preparation of plasmid DNA, restriction enzyme digestion, agarose gel electrophoresis of DNA, and other molecular biology methods were adapted from Sambrook et al., 1989. C. elegans culture methods were adapted from Brenner, 1974, and nematode DNA isolation was adapted from Sulson and Hodgkins, 1988.

Transgenic Strains

Plasmid IM#58, carrying *unc-6(+)*, contains a 9643 bp ClaI-EcoRI insert, subcloned from λ phage NJ#14, in the vector pBluescript II SK(+). The insert includes the protein coding region of *unc-6(+)* plus some 1500 bp of 5′ and 1254 bp of 3′ flanking sequences (Ishii et al., 1992). Plasmid IM#94, carrying *unc-6::HA*, was constructed from UR#58 by PCR methods. In brief, a unique *BglI* site was created in the protein coding region immediately following the predicted UNC-6 signal peptide. A 123 bp BglI fragment, encoding three tandem copies of the HA-epitope recognized by mAb 12CA5, was then ligated into this site (Field et al., 1988). By design, the reading frame was maintained.

Transgenic strains were obtained by microinjecting plasmid DNA (10 μg/ml) into the ovaries of *unc-6* (*ev400*) hermaphrodites (Fire, 1986; Mello et al., 1991). Progeny inheriting and expressing *unc-6(+)* or *unc-6::HA* were identified by their wild-type locomotion and propagated individually. Three independent strains were established using plasmid UR#58. Similarly, four independent strains were established using UR#94. From one of these strains carrying *unc-6::HA* as an extrachromosomal array, an integrated transgene, *unc-6::HA (urIs1)*, was obtained using a γ-irradiation protocol (C. Kari et al., personal communication).

Immunohistochemistry

Gravid *unc-6::HA (urIs1)* hermaphrodites were harvested in distilled water and then suspended in hypochlorite solution (1N NaOH, 10% bleach) for two washes of about 3 min each, until larvae and adults were dissolved. After one rinse with distilled water, the eggs were pipetted (10–15 μl) onto polylysine-coated glass slides and covered with a glass coverslip. To freeze the slides, they were placed on an aluminum block that had been prechilled with liquid nitrogen. After removing the coverslips, the frozen slides were fixed immediately by immersion in cold methanol (approximately −20°C) for 2 min followed by cold acetone for another 4 min. The fixed slides were allowed to dry at room temperature before incubation with antibodies.

For UNC-6::HA staining, slides were overlaid with monoclonal antibody 12CA5 (Boehringer Mannheim) in TTBS (100 mM Tris [pH 7.4], 200 mM NaCl, 0.1% Tween-20). After overnight incubation in a humidified chamber at 4°C, slides were washed four times in phosphate buffered saline (PBS) and then dipped into TTBS. The secondary antibody, FITC-conjugated anti-mouse IgG (Boehringer Mannheim), was applied (1:1000 in TTBS) for 2 hr. Finally, the slides were dipped in propidium iodide (5 μg/ml in PBS), rinsed three times in PBS, and then mounted in FITC-Guard (Testog). For double labeling, monoclonal antibody OIC1D4 (Strome and Wood, 1982; Strome, 1986) or MH27 (Priess and Hirsh, 1986; Podbilewicz and White, 1994) was added during the first incubation. Confocal images were collected on a confocal laser scanning microscope (Molecular Dynamics). Strains lacking the *unc-6::HA* transgene were used as negative controls. Monoclonal antibody M44 is a mouse IgG1, generated by immunization with C. elegans homogenates, that reacts with a cell surface antigen on the PVP neurons (H. Bhatt and E. Hedgecock, unpublished data).

PCR Amplification and Single Strand Conformation Polymorphism Analysis

For each mutant allele, overlapping PCR products covering the entire coding region of the gene were generated. Each product was analyzed by single strand conformation polymorphism (Orita et al., 1989a, 1989b) to detect nucleotide changes. PCR products suspected of containing changes were cloned into pBluescript vectors (Stratagene). Single-stranded DNA from at least 3 individual subclones were sequenced by the dideoxy chain termination method using the Sequenase system (United States Biochemical Corporation).

cDNA Cloning and Sequencing

To analyze the structure of *unc-6* mRNAs, RNA/DNA was prepared from worms homozygous for the *rh69*, *rh202*, *rh204*, and *rh402* alleles as described (Villeneuve and Meyer, 1987), except that the initial extraction was by freezing the nematode pellet at −80°C for 1 hr, adding guanidine isothiocyanate solution, and vortexing hard for 5 min. The RNA/DNA preparation was resuspended in 20 μl RNase-free Tris-EDTA (pH 7.4) with 500 ng of poly A primer, incubated at 65°C for 4 min, and cooled on ice. cDNA was synthesized in a 50 μl reaction by incubating the preparation at 37°C for 30 min with 800 U of M-MLV Reverse Transcriptase (Life Technologies) under the conditions recommended by the manufacturer. PCR amplification of the cDNA was performed using primers annealing to sequences of exons 5 and 8. The products were analyzed by agarose gel electrophoresis, subcloned, and sequenced. At least 3 individual subclones representing a single allele were sequenced.

Restriction Fragment Polymorphisms

Deletions were detected as restriction fragment length polymorphisms by Southern blot analysis (Sambrook et al., 1989). Genomic DNA (10 μg) was prepared from animals homozygous for the wild type, *rh201*, *rh202*, *rh203*, *rh204* and *rh402 unc-6* alleles and was digested with PstI, HindIII, or Sau3A. The resulting fragments were separated on 0.8% or 1.2% (for Sau 3A fragments) agarose gels and blotted to Optibind (Schleicher and Schuell). For hybridizations, digoxigenin-labeled DNA probes corresponding to the entire *unc-6* gene were synthesized using the Genius kit (Boehringer Mannheim).

Acknowledgments

Address correspondence to W. G. W. We thank Ross Francis, Susan Strome, and Robert Waterston for providing monoclonal antibodies; Monica Driscoll, Gautam Kao, Carolyn Norris, Jochen Scheel, and Jeffery Way for comments on the manuscript; Ruth Steward and Richard Leidich for advice in confocal microscopy (Waksman Institute of Rutgers University); Donald Winkleman and David Foran of the Robert Wood Johnson Medical School Bioimaging Laboratory for help in preparing micrographs; and members of our laboratories for useful discussions. This study was supported by grants from the Foundation of the University of Medicine and Dentistry of New Jersey (W. G. W.) and the National Institutes of Health (NS33156, W. G. W; NS26295, E. M. H).

The costs of publication of this article were defrayed in part by the payment of page charges. This article must therefore be hereby marked ''*advertisement*'' in accordance with 18 USC Section 1734 solely to indicate this fact.

Received July 14, 1995; revised September 20, 1995.

References

Albertson, D., and Thomson, J. (1976). The pharynx of *Caenorhabditis elegans*. Phil. Trans. R. Soc. Lond. (B) *275*, 299–325.

Beck, K., Hunter, I., and Engel, J. (1990). Structure and function of laminin: anatomy of a multidomain glycoprotein. FASEB J. *4*, 148–160.

Brenner, S. (1974). The genetics of *Caenorhabditis elegans*. Genetics *77*, 71–94.

Colamarino, S.A., and Tessier-Lavigne, M. (1995). The axonal chemoattractant netrin-1 is also a chemorepellent for trochlear motor axons. Cell *81*, 621–629.

Durbin, R. (1987). Studies on the development and organisation of the nervous system of *Caenorhabditis elegans*. PhD thesis, University of Cambridge, England.

Field, J., Nikawa, J.-I., Broek, D., MacDonald, B., Rodgers, L., Wilson, I., Lerner, R., and Wigler, M. (1988). Purification of a RAS-responsive adenylyl cyclase complex from *Sacchromyces cerevisiae* by use of an epitope addition method. Mol. Cell. Biol. *8*, 2159–2165.

Fire, A. (1986). Integrative transformation of *Caenorhabditis elegans*. EMBO J. *5*, 2673–2680.

Hamelin, M., Zhou, Y., Su, M.-W., Scott, I.M., and Culotti, J.G. (1993). Expression of the UNC-5 guidance receptor in the touch neurons of *C. elegans* steers their axons dorsally. Nature *364*, 327–330.

Hedgecock, E., Culotti, J., David, H., and Stern, B. (1987). Genetics of cell and axon migrations in *Caenorhabditis elegans*. Development *100*, 365–382.

Hedgecock, E.M., Culotti, J.G., and Hall, D.H. (1990). The *unc-5, unc-6,* and *unc-40* genes guide circumferential migrations of pioneer axons and mesodermal cells on the epidermis in C. elegans. Neuron *4*, 61–85.

Hynes, R.O., and Lander, A.D. (1992). Contact and adhesive specificities in the association, migrations, and targeting of cells and axons. Cell *68*, 303–322.

Ishii, N., Wadsworth, W.G., Stern, B.D., Culotti, J.G., and Hedgecock, E.M. (1992). UNC-6, a laminin-related protein, guides cell and pioneer axon migrations in C. elegans. Neuron *9*, 873–881.

Jacobson, M. (1991). Developmental Neurobiology. (New York: Plenum Press).

Kennedy, T.E., Serafini, T., de la Torre, J., and Tessier-Lavigne, M. (1994). Netrins are diffusible chemotropic factors for commissural axons in the embryonic spinal cord. Cell *78*, 425–435.

Leung-Hagesteijn, C., Spence, A.M., Stern, B.D., Zhou, Y., Su, M.W., Hedgecock, E.M., and Culotti, J.G. (1992). UNC-5, a transmembrane protein with immunoglobulin and thrombospondin type 1 domains, guides cell and pioneer axon migrations in C. elegans. Cell *71*, 289–299.

Mello, C.C., Kramer, J.M., Stinchcomb, D., and Ambros, V. (1991). Efficient gene transfer in *C. elegans*: extrachromosomal maintenance and integration of transforming sequences. EMBO J. *10*, 3959–3970.

Orita, M., Iwahana, H., Hayashi, K., and Sekiya, T. (1989a). Detection of polymorphisms of human DNA by gel electrophoresis as single-strand conformation polymorphisms. Proc. Natl. Acad. Sci. USA *86*, 2766–2770.

Orita, M., Suzuki, Y., Sekiya, T., and Hayashi, K. (1989b). Rapid and sensitive detection of point mutations and DNA polymorphisms using the polymerase chain reaction. Genomics *5*, 874–879.

Podbilewicz, B., and White, J.G. (1994). Cell fusions in the developing epithelia of *C. elegans*. Dev. Biol. *161*, 408–424.

Priess, J., and Hirsh, D. (1986). *Caenorhabditis elegans* morphogenesis: the role of the cytoskeleton in the elongation of the embryo. Dev. Biol. *117*, 156–173.

Sambrook, J., Fritsch, E.F., and Maniatis, T. (1989). Molecular Cloning: A Laboratory Manual (Cold Spring Harbor, New York: Cold Spring Harbor Laboratory Press).

Schittny, J.C., and Yurchenco, P.D. (1990). Terminal short arm domains of the basement membrane protein laminin are critical for its self-assembly. J. Cell Biol. *110*, 825–832.

Serafini, T., Kennedy, T.E., Galko, M.J., Mirzayan, C., Jessell, T.M., and Tessier-Lavigne, M. (1994). The netrins define a family of axon outgrowth-promoting proteins homologous to C. elegans UNC-6. Cell *78*, 409–424.

Strome, S. (1986). Asymmetric movements of cytoplasmic components in *Caenorhabditis elegans* zygotes. J. Embryol. Exp. Morph. *97*, 15–29.

Strome, S., and Wood, W.B. (1982). Immunofluorescence visualization of germ-line-specific cytoplasmic granules in embryos, larvae, and adults of *Caenorhabditis elegans*. Proc. Natl. Acad. Sci. USA *79*, 1558–1562.

Sulston, J., Schierenberg, E., White, J., and Thomson, J. (1983). The embryonic cell lineage of the nematode *Caenorhabditis elegans*. Dev. Biol. *78*, 577–597.

Tessier-Lavigne, M., Placzek, M., Lumsden, A.G.S., Dodd, J., and Jessell, T.M. (1988). Chemotropic guidance of developing axons in the mammalion central nervous system. Nature *336*, 775–778.

Villeneuve, A.M., and Meyer, B.J. (1987). *sdc-1*; a link between sex determination and dosage compensation in *C. elegans*. Cell *48*, 25–37.

Wadsworth, W.G., and Hedgecock, E.M. (1992). Guidance of neuroblast migrations and axonal projections in *Caenorhabditis elegans*. Curr. Opin. Neurobiol. *2*, 36–41.

White, J., Southgate, E., Thompson, J., and Brenner, S. (1986). The structure of the nervous system of the nematode *Caenorhabditis elegans*. Phil. Trans. R. Soc. Lond. (B) *314*, 1–340.

Yurchenco, P.D., and Cheng, Y.S. (1993). Self-assembly and calcium-binding sites in laminin: a three-arm interaction model. J. Biol. Chem. *268*, 17286–17299.